Tuning of Photo- and Electroluminescence of New Soluble, PPV-Analogous Short-Chain Compounds with Naphthalene Moieties

P. Martinez-Ruiz,[a] B. Behnisch,[a] K.-H. Schweikart,[a] M. Hanack,*[a] L. Lüer,[b] and D. Oelkrug*[b]

Abstract: A series of oligomers analogous to poly(*p*-phenylenevinylene) (PPV), combining naphthalene and benzene as aromatic units, have been synthesized by a Knoevenagel reaction. By measuring UV/Vis spectra, photoluminescence (PL) and electroluminescence (EL), we studied the influence of the position of the naphthalene unit as well as the steric and electronic influences of cyano and alkyloxy substituents on the luminescent properties of these compounds.

Keywords: conjugation · fluorescence spectroscopy · luminescence · organic light-emitting diodes · phthalocyanines · polymers

Introduction

Poly(*p*-phenylenevinylene) (PPV) and other related π-conjugated polymers and oligomers have attracted increasing attention in recent years owing to their application as light-emitting layers in organic light-emitting diodes (OLEDs).[1] These materials offer the possibility of tuning both the characteristics of the emitted light and the efficiency of the devices by means of simple chemical modification of their structure. The most commonly followed strategies for chemical modification consist of a) the introduction of lateral chains that can improve the solubility of the compounds and effect the conjugation of the system by steric hindrance,[2] b) the introduction of electron-withdrawing substituents, such as cyano groups, which increase the electron affinity of the molecules[3] or c) the replacement of the phenylene ring by other aromatic structures.[4] We have previously reported the synthesis of the substituted poly-2,6-naphthylenevinylene (PNV) **2** and the corresponding phenylene/naphthylene copolymer **3** (Figure 1).[5, 6] Polymer **2** shows a strong shift in the photoluminescence (PL) maximum to a shorter wavelength relative to the phenylene-based compound **1**, which is a good emitting layer in OLEDs.[7] The PL maximum of copolymer **3**, which contains stoichiometrically alternating benzene and naphthalene units, has an intermediate value between those of compounds **1** and **2**.[6]

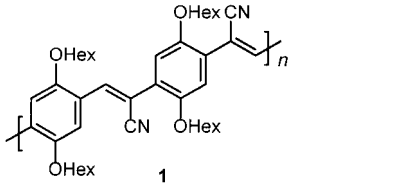

1

PL = 710 nm

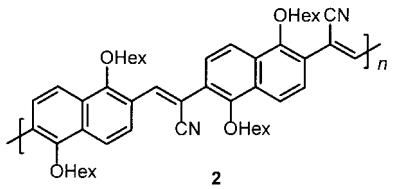

2

PL = 500 nm

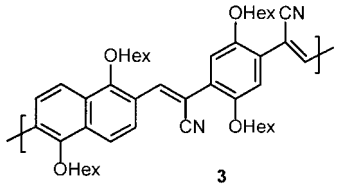

3

PL = 595 nm

Figure 1. Structures and photoluminescence (PL) maxima of PPV and 2,6-PNV derivatives.

These results seem to contradict those of a previous work on the luminescence of PPV copolymers that contain randomly distributed phenylene and naphthylene units.[8] The authors have indicated that the presence of naphthalene moieties conjugated in 2,6-positions did not significantly change the structure of the band gap and therefore the luminescence of the polymer was little affected. On the other hand, naphtha-

[a] Prof. Dr. M. Hanack, Dr. P. Martinez-Ruiz, B. Behnisch, K.-H. Schweikart
Institut für Organische Chemie Lehrstuhl II
Universität Tübingen, Auf der Morgenstelle 18
72076 Tübingen (Germany)
Fax: (+49) 7071-29-5244
E-mail: hanack@uni-tuebingen.de

[b] Prof. Dr. D. Oelkrug, L. Lüer
Institut für Physikalische Chemie
Universität Tübingen, Auf der Morgenstelle 8
72076 Tübingen (Germany)

0947-6539/00/0608-1294 $ 17.50+.50/0 *Chem. Eur. J.* **2000**, *6*, No. 8

lene units linked in 1,4-positions provoke a red shift due to a decrease in the band gap of the polymer.[9]

The study of a reproducible set of properly characterized and well-defined, conjugated oligomers as model compounds for related conjugated polymers helps us to understand the structure–property relationship. These short-chain compounds can also be useful in their own right as light-emitting layers as a result of high-vacuum deposition techniques, which allow the preparation of high quality films.

With this in mind, we have previously reported the synthesis of different phenylene- and naphthylenevinylene oligomers.[10] Comparison of the photoluminescence spectra of these model compounds indicates that replacement of the central phenylene moiety by naphthylene leads to a blue shift in the emitted light.[10a] A hypsochromic effect has also been observed on increasing the steric hindrance by varying the position of cyano groups attached to the vinylene linkages. In species **6** (Figure 2) the cyano group is linked to the vinylene carbon neighbouring the central phenylene ring (α-positions); this results in steric and electronic interaction with the hexyloxy chains. Thus, the PL maximum of species **6** is shifted more than 100 nm to the blue with regard to that of compound **5**, in which the cyano group has no interaction with the hexyloxy groups (β-positions).[10b] The steric influence due to molecular torsion has been confirmed by determining the crystal structure of a related compound.[11]

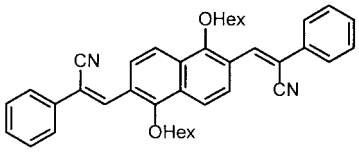

4

PL = 555 nm

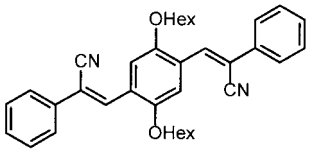

5

PL = 595 nm

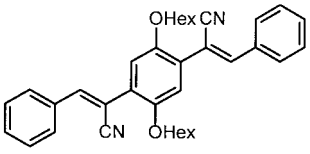

6

PL = 479 nm

Figure 2. Structures and PL maxima of short-chain PPV-analogous model compounds.

Abstract in German: *Die systematische Synthese und Charakterisierung von acht neuen PPV-analogen Modell-Verbindungen mit photo- und elektrolumineszenten Eigenschaften ist Thema dieser Arbeit. Besonderes Interesse liegt auf der Untersuchung der sterischen und elektronischen Einflüsse von Cyano-Gruppen und Hexyloxy-Ketten an den Phenyl- und Naphthyl-Einheiten des konjugierten Systems. Durch Variation dieser Reste können die optischen Eigenschaften dieser Verbindungen stark modifiziert werden.*

Results and Discussion

Little research has been undertaken on short-chain PPV derivatives whose structure can be compared with that of the polymers **1**–**3**. Therefore, we have synthesized a series of new cyano-substituted PPV-analogous compounds (species **21**–**28**, Figure 3), by combining both 1,4-benzene and 2,6-naphthalene moieties with six hexyloxy substituents that provide for excellent solubility in common organic solvents and good film-forming properties. The new compounds have been characterized by IR, ^{1}H and ^{13}C NMR spectroscopy and mass spectrometry (MS). The optical properties were studied by measuring UV-visible spectra in CH_2Cl_2 solution, photoluminescence (PL) in the solid state and electroluminescence (EL) in double-layer devices with copper phthalocyanine (PcCu) as a convenient and thermally stable hole-transporting layer[12] and aluminium as an air-stable cathode (ITO/PcCu/emitter **21**–**28**/Al). From the wavelengths of the maxima of absorption and emission spectra, we can evaluate the influence exerted by naphthalene rings and cyano groups in different positions, as well the effect on these constituents of neighbouring hexyloxy chains.

To prepare the new model compounds **21**–**28**, we combined eight different precursor molecules by a Knoevenagel reaction (Scheme 1). For the central units, the dialdehydes **7** and **9** and the cyanomethylene derivatives **8** and **10** were used; these were synthesized from hydroquinone and 1,5-dihydroxynaphthalene as previously described.[5, 7] As starting materials for compounds **23**, **24**, **27** and **28** the 1,4-dihexyloxynaphthalenes **11** and **12** have been chosen.

The preparation of the monofunctionalized end-unit precursors **11**, **12**, **13** and **14** is shown in Scheme 2. Alkylation of 1,4-dihydroxynaphthalene (**19**) with *n*-hexyl bromide, followed by reaction with dichloromethyl methyl ether in the presence of $TiCl_4$[13] gives exclusively monoaldehyde **11**. This two-step procedure also allows the synthesis of aldehyde **13** from hydroquinone. On the other hand, alkylation and bromomethylation of **19**[14] yields the bromomethylene derivative **20**, which on reaction with tetrabutylammoniumcyanide gives cyanomethylene compound **12**. Synthesis of phenylacetonitrile **14** from 2-methylhydroquinone (**17**) was achieved in three steps by alkylation, bromination with NBS and finally reaction with tetrabutylammoniumcyanide in methylene chloride (Scheme 2).

1,4-Dihexyloxynaphthalene derivatives **11** and **12** were used as precursors owing to their ease of preparation. Oligomers obtained from the former should serve as model compounds for studying the properties of polymers **2** and **3** (Figure 1). The new target compounds **21**–**28** synthesized by the Knoevenagel reaction are shown in Figure 3, grouped in two series depending on the central moiety.

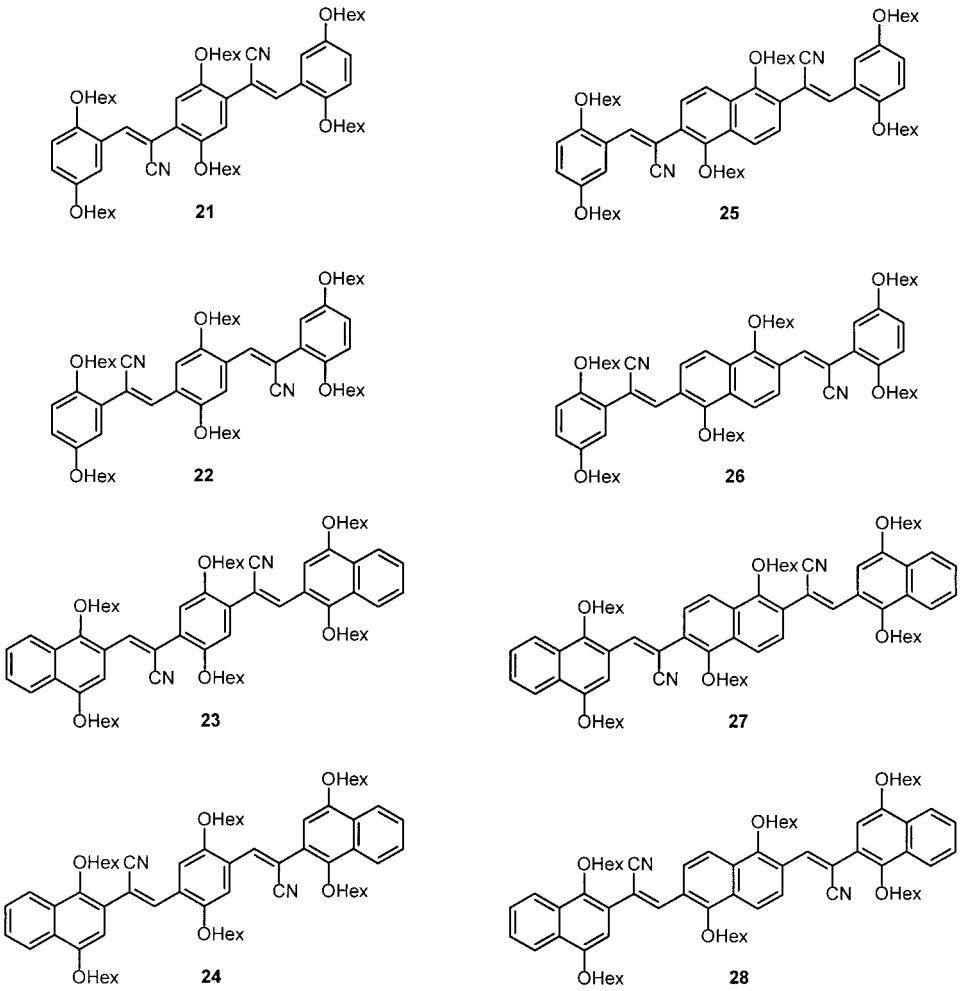

Figure 3. Structures of the new Knoevenagel products **21**–**28**.

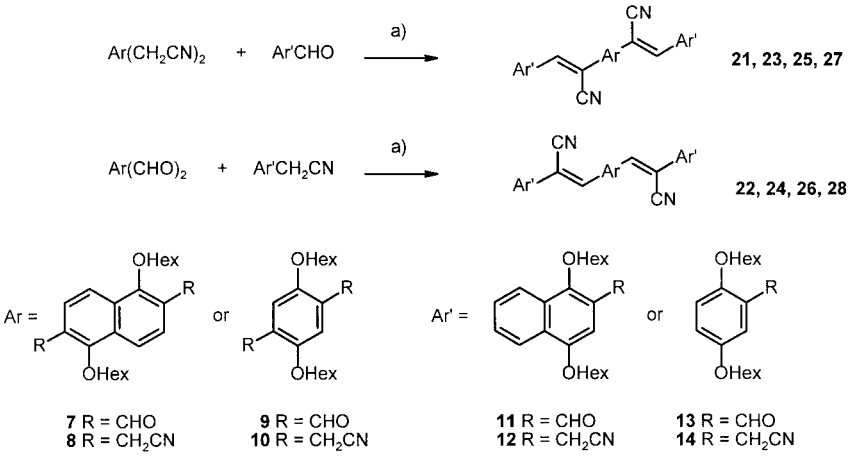

Scheme 1. Synthesis of the new Knoevenagel condensation products **21**–**28**. a) *t*BuOK/$(n\mathrm{Bu})_4$NOH, THF/*t*BuOH.

described roughly as a linear superposition of the π-donating and π-accepting molecular fragments.[15] The band maxima of the HOMO–LUMO transitions are given in Table 1.

Alkoxy substituents $(RO)_n$ in 2,5-positions of the phenyl rings, as in **21**–**24**, reduce the energy of the first π–π* transition by approximately $-\Delta\nu = 3000-3500\ \mathrm{cm}^{-1}$ (≈ 0.4 eV) from that of unsubstituted PV.[16] The reduction can be explained by the interaction of the occupied PV π orbitals of the alkoxy substituents with the HOMO of the conjugated backbone; this leads to an elevation of the HOMO energy, whereas the LUMO energy is not changed significantly. Semiempirical quantum-chemical MO calculations confirm these results. By using the Pariser–Parr–Pople SCF method (PPP), we obtain $-\Delta\nu = 3200\ \mathrm{cm}^{-1}$, and with the ZINDO/S method $-\Delta\nu = 1700\ \mathrm{cm}^{-1}$ was obtained. These results are presented in Table 1 along with the HOMO and LUMO energies.

Additional introduction of cyano substituents in the *β*-positions of the vinylene groups, such as in **22** and **24**, also shift the $S_0 \rightarrow S_1$ transition to the red, because the LUMO energy is lowered further by coupling with the anti-bonding π* orbitals of the cyano groups than the HOMO energy. The experimental value of $\Delta\nu = -1000\ \mathrm{cm}^{-1}$ is somewhat lower than the ZINDO/S result of $\Delta\nu = -2000\ \mathrm{cm}^{-1}$ and the PPP result of $\Delta\nu = -3200\ \mathrm{cm}^{-1}$. Theoretically, cyano substituents in *α*-positions should also create red-shifted $S_0 \rightarrow S_1$ absorption bands. However, the experiments show that the band positions are shifted to the blue. This effect is not yet fully understood. It may be a result of the sterically induced non-planarity of the central phenylene-vinylene system,[16] which reduces the effective conjugation length of the trimer and thus raises the HOMO–LUMO energy gap. It must be stressed that all calculations were performed on planar geometries.

UV-visible absorption spectra: Figure 4 and Figure 5 show dilute solution spectra of compounds **21** and **22** with three phenyl units (**ppp**) and their naphthyl analogues **23**–**28** with one central (**pnp**), two peripheral (**npn**) and three naphthyl units (**nnn**). For comparison the spectrum of unsubstituted trimeric phenylene-vinylene (PV) is also displayed. The correlation between chemical structure and spectrum can be

0947-6539/00/0608-1296 $ 17.50+.50/0 *Chem. Eur. J.* **2000**, *6*, No. 8

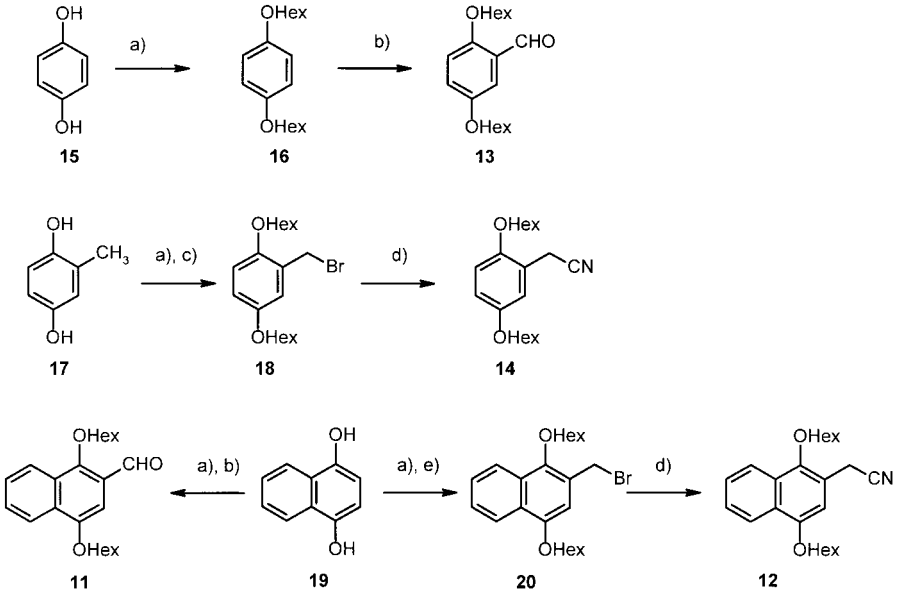

Scheme 2. Synthesis of the end-unit precursors **11** to **14**. a) *n*-Hexyl-Br, EtOH, Δ; b) $Cl_2HCOCH_3/TiCl_4$, CH_2Cl_2; c) NBS, CCl_4, Δ; d) $(n\mathrm{Bu})_4\mathrm{NCN}$, CH_2Cl_2; e) HBr/AcOH, AcOH.

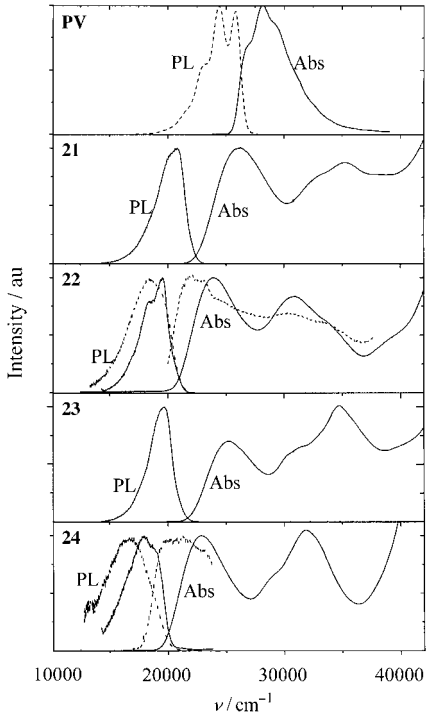

Figure 4. UV-visible absorption spectra in CH_2Cl_2 solution and PL spectra of thin films of the compounds **21**–**24** and PV (smooth lines). For PV, **22** and **24** fluorescence spectra in solution and for **22** and **24** fluorescence excitation spectra in thin films are given (dashed lines).

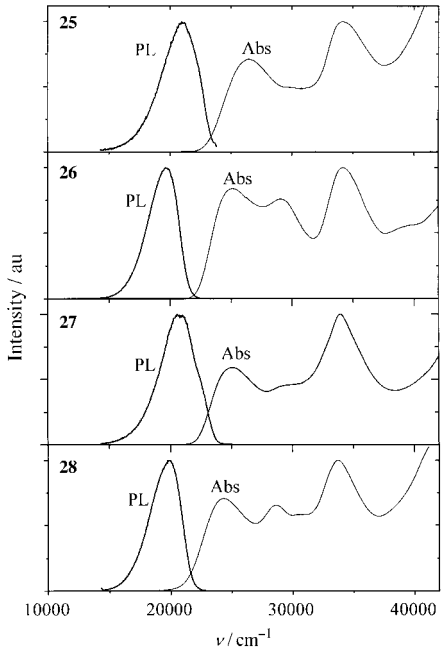

Figure 5. UV-visible absorption spectra in CH_2Cl_2 solution and PL spectra of thin films of the compounds **25**–**28**.

Replacing the phenyl substituents by naphthyl substituents would be intuitively expected to reduce the $S_0 \rightarrow S_1$ transition energy, since the effective polyene-like conjugation in the direction of the long molecular axis becomes longer by one −C=C− unit per naphthalene group. The ZINDO/S HOMO–LUMO energy differences support this intuition. The values relative to PV are $\Delta E = -0.13$, -0.22 and -0.29 eV for **pnp** (**25**, **26**), **npn** (**23**, **24**) and **nnn** (**27**, **28**), respectively. However, the calculated $S_0 \rightarrow S_1$ transition energies are only $\Delta E = 0$ to -0.1 eV lower, since the smaller HOMO–LUMO energy gaps are almost completely compensated for by the reduction of the interelectronic repulsion energies in the corresponding S_1 states. A blue shift, however, can be calculated if one allows ring torsion during geometrical optimization. The experimental blue shift can thus be explained by a substantial torsion of the phenylene planes against the vinylene planes.

Figure 6 displays the superimposed contributions of alkoxy, cyano and naphthyl groups to the positions of the experimental $S_0 \rightarrow S_1$ absorption maxima of the PV derivatives **21**–**28**. The whole series of *β*-cyano compounds, in which the cyano groups are bound close to the terminal aromatic rings, is red-shifted against $(RO)_6$PV without cyano substituents. However, the *α*-cyano derivatives are blue-shifted against the $(RO)_6$PV, contrary to theoretical predictions. The band positions of the naphthalene analogues in the *β*-cyano series can be interconnected by an almost perfect correlation parallelogram. Thus, replacement of the central phenylene group by a naphthylene group creates a substantial blue shift that is independent of the chemical nature of the peripheral aromatic rings, $\Delta E(\mathbf{pnp} - \mathbf{ppp}) = \Delta E(\mathbf{nnn} - \mathbf{npn}) = +1400\ \mathrm{cm}^{-1}$. As stated above, this blue shift is explained by ring torsion.

Table 1. Electronic properties of substituted 1,4-distyrylbenzenes. The HOMO and LUMO energies as well as the lowest singlet transitions are calculated by ZINDO/S SCI from AM1-optimized structures. Values for PV are given absolutely. All other calculated values are differences between the values calculated for the compound and that of the unsubstituted compound PV. The calculated values for **21**–**28** are the sums of the contributions of individual substituents.

	calculated energies			experimental band maxima		
compound	E_{HOMO} [eV]	E_{LUMO} [eV]	$E(S_0 \rightarrow S_1)$ [cm^{-1}]	E_{max} [cm^{-1}] exptl	λ(UV/Vis) [nm]	$\varepsilon_{0\rightarrow1}$ [$M^{-1}cm^{-1}$]
PV ≅ ppp	−7.11	−0.54	28800	28800	355	60000
model compounds			energy differences compared with **PV**			
$(RO)_6$ppp	+0.26	+0.06	−1700	−3300	402	40000
α-$(CN)_2$ppp	−0.46	−0.62	−800	+4800	300	–
β-$(CN)_2$ppp	−0.48	−0.79	−2000	+100	353	–
pnp	+0.07	−0.06	0			
npn	+0.12	−0.1	−900			
nnn	+0.16	−0.13	−800			
β-cyano						
ppp **22**	−0.22	−0.73	−3700	−4300	418	26000
pnp **26**	−0.15	−0.79	−3700	−3100	399	27000
npn **24**	+0.03	−0.83	−4600	−5400	438	30000
nnn **28**	−0.06	−0.86	−4500	−3900	411	37000
α-cyano						
ppp **21**	−0.20	−0.56	−2500	−2100	384	22000
pnp **25**	−0.13	−0.62	−2500	−1800	379	23000
npn **23**	+0.05	−0.66	−3600	−3000	397	31000
nnn **27**	−0.04	−0.69	−3300	−3100	398	38000

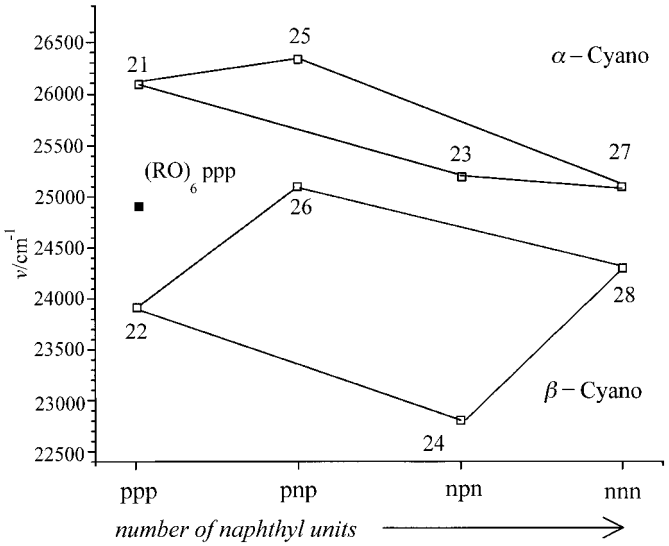

Figure 6. Correlation parallelograms of the absorption maxima of the PV derivatives **21**–**28**.

On the other hand, replacement of the peripheral phenyl groups by naphthyl groups creates a red shift that is independent of the chemical nature of the central aromatic ring, $\Delta E(\mathbf{npn} - \mathbf{ppp}) = \Delta E(\mathbf{nnn} - \mathbf{pnp}) = -1000\ cm^{-1}$. This result is approximately in accord with model predictions (see Table 1).

In addition to the band positions, the oscillator strengths and maximum extinction coefficients ε_{max} of the $S_0 \rightarrow S_1$ transition change appreciably with chemical substitution. In the parent PV the oscillator strength of the low-lying $\pi-\pi^*$ transition is mainly localized in $S_0 \rightarrow S_1$ with $\varepsilon_{max} = 60000\ M^{-1}cm^{-1}$. This transition is polarized in the direction of the long molecular axis. Introduction of substituents in the 2,5-positions of the phenyl rings changes the orientation of the HOMO and creates a linear combination with lower lying orbitals that were originally concentrated almost exclusively in the phenyl rings. Thus, the higher energy $S_0 \rightarrow S_n$ transitions gain intensity at the expense of $S_0 \rightarrow S_1$. This can be clearly seen in $(RO)_6$PV, for which a second band with $\varepsilon = 15000\ M^{-1}cm^{-1}$ appears at the expense of the first band, whose extinction coefficient is reduced to $\varepsilon = 40000\ M^{-1}cm^{-1}$. Upon CN substitution the effect is even more pronounced, and in the naphthalene analogues the higher transitions become substantially more intense than the $S_0 \rightarrow S_1$ transition. These results have consequences for the intrinsic fluorescence lifetimes that increase from $\tau_0 = 2.1$ ns ($(RO)_6$PV) to $\tau_0 = 5$ ns (β-cyano-$(RO)_6$PV, **22**), and also indirectly influence the fluorescence quantum yields, since non-radiative pathways compete more efficiently with the radiative ones in long-lived electronic systems.

Photoluminescence: The parent PV is a bright blue-violet emitter in dilute solution with a fluorescence quantum yield close to unity ($\phi_F > 0.9$), but only a poor one in vapour deposited or spin-cast films ($\phi_F < 0.1$).[16] This is because in adjacent PV molecules close side-by-side aggregates are formed, which, according to the exciton model, make the lowest excited state optically forbidden. Moreover, the formation of charge-separated states is enhanced. Thus, it is necessary to be sure that substituents are suitable for avoiding side-by-side aggregation, while taking care that these substituents do not create new intramolecular nonradiative pathways.

In dilute solutions, the fluorescence yields of cyano-substituted PV polymers are distinctly lower than those of PV itself.[16] Also, in contrast to PV, the solution fluorescence spectra show no vibronic resolution (compare Figure 4, dashed lines), even in rigid solvents. This result is typical for phenylene-like molecules than cannot become planar in the quinoidal S_1-state owing to the steric hindrance of bulky substituents.

0947-6539/00/0608-1298 $ 17.50+.50/0 *Chem. Eur. J.* **2000**, *6*, No. 8

In films and crystals of the β-cyano compounds, the Stokes shifts are much less pronounced than in solution. The $S_0 \rightarrow S_1$ absorption bands are red-shifted by $-\Delta\nu = 1000-1500\ cm^{-1}$ ($\Delta\lambda \approx 25-30$ nm), due to the higher polarizabilities of the solids and possibly also due to their less twisted geometries and correspondingly lower HOMO–LUMO gaps. The fluorescence bands, however, are blue-shifted by $+\Delta\nu = 1000-1500\ cm^{-1}$, indicating suppression of the wide-amplitude torsional modes around the φ-C(CN) bond. Comparable fluorescence blue shifts resulting from intermolecular interactions have not yet been observed in phenylene-vinylene oligomers. On the contrary, trimers similar to **22**, but without peripheral alkoxy substituents, exhibit extremely red-shifted fluorescence spectra originating from a low-energy shoulder in the absorption spectrum. Also, in polymers strongly red-shifted fluorescence spectra have been reported.[17] These spectral features have been assigned to interchain transitions in aggregates with strong $\pi-\pi$ overlap. The aggregates can form excimers with strongly red-shifted fluorescence bands and long fluorescence lifetimes ($\tau_F \approx 30$ ns) that exceed the lifetimes usually observed in PVs by more than one order of magnitude. Additional alkoxy groups reduce intermolecular $\pi-\pi$ overlap. The blue shift of the excitonic fluorescence spectra is thus no longer masked by excimer fluorescence.

The fluorescence quantum yields in the solid state are not substantially changed upon substitution. From powder samples of **22**, **24** and PV, relative quantum yields were measured to be $\phi_{F,rel} = 1.4$, 0.6 and 1, respectively.

Electroluminescence: For the investigation of the electroluminescence (EL) properties of the synthesized compounds **21**–**28** we prepared devices that contain 25 segments for screening-tests. Each segment can be driven separately. For the patterning of the devices, commercially available glass-ITO substrates were structured by a method described earlier by our group.[18]

Due to the electron-conducting properties of short-chain PPV derivatives, the application of these emitters in single-layer arrangements produced no measurable electroluminescence. However, by introducing an additional hole-transporting layer, the compounds became capable of display applications. One of the most common hole-transporting layers is the thermally stable copper phthalocyanine (PcCu).[12] All synthesized PPV-analogous compounds **21**–**28** showed electroluminescence in an ITO/PcCu/emitter/Al configuration. The wavelengths of the emission maxima are listed in Table 2. The colours ranged from blue-green for **21** to yellow for **24**. The EL spectra of compounds **21**, **24** and **28** are displayed together with the corresponding PL spectra in Figure 7. The EL spectra reflect the corresponding fluorescence spectra in thin films.

Table 2. Comparison of the photoluminescence (PL) and electroluminescence (EL) maxima of compounds **21**–**28**.

	λ(PL) [nm]	λ(EL) [nm]
21	485	479
22	512	514
23	510	503
24	560	535
25	477	510
26	510	510
27	482	513
28	506	515

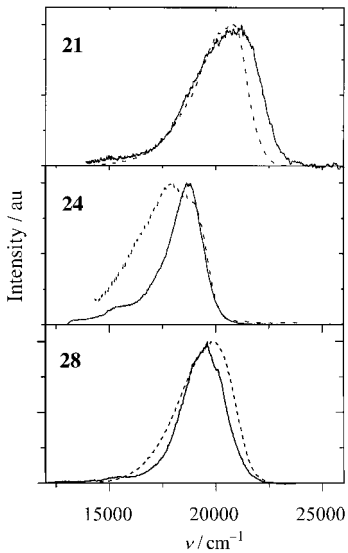

Figure 7. Comparison of the PL (dashed lines) and EL (smooth lines) spectra of compounds **21**, **24** and **28**.

Therefore, it is possible to tune the emitted light by undertaking theoretical calculations and measurements of thin-film photoluminescence spectra. The difference of more than 25 nm between the maxima in the EL and PL spectra for the yellow-emitting device of **24** can be explained by absorption of the red part of the emission by the PcCu layer, which shifts the maximum to a shorter wavelength. This effect can be suppressed by using a thinner film of PcCu or by using different phthalo- or naphthalocyanines with absorption bands in the near-IR region. The intensity of the emitted light is strongly dependent on the device preparation, especially layer thickness, driving voltage, film characteristics (e.g., pinholes, aggregation effects, impurities) and vacuum conditions. Hence, a quantitative comparison of the intensity of the devices was not within the scope of this work, but is under investigation.

Conclusion

We have synthesized eight new soluble hexaalkoxy-dicyano-substituted PPV-analogous compounds **21**–**28** with different combinations of naphthyl and phenyl units and investigated their optical and electroluminescence properties. All the compounds are highly soluble in common solvents allowing them to be spin-cast into thin films. The thermal stability of the compounds is sufficient for vapour deposition, so that films of high purity can be processed. All compounds show electroluminescence in ITO/PcCu/emitter/Al devices. The maxima of UV-visible, PL and EL spectra depend strongly on the type and position of the aromatic units and both the steric and electronic influences of the cyano groups. Peripheral

naphthyl units shift the maxima to the red, central naphthylene units to the blue, when compared with the analogous phenylenic units. These findings were rationalized on the basis of semiempirical calculations. The spectral shifts induced by the nature of the peripheral aromatic units are explained by alterations in the HOMO – LUMO gap, whereas the blue shift upon naphthylene substitution of the central phenylene unit is explained by an increase in the average torsion angle between the aromatic and the vinylene plane. The new compounds are useful candidates in the search for materials that will lead to a better understanding of the relationship between structure and luminescence.

Experimental Section

Spectroscopy: ^{1}H and ^{13}C NMR spectra were recorded on a Bruker ARX250 with TMS as an internal standard. FT-IR spectra were recorded on a Bruker IFS48 as KBr pellets. UV/Vis spectra were taken in dichloromethane with a Perkin – Elmer Lambda2 spectrophotometer. Fluorescence of evaporated films was measured with a SPEX fluorolog 112 in the 45° configuration. For the preparation of the light-emitting diodes, glass-ITO substrates were specially structured by a method described by our group earlier.[18] After cleaning the device, a thin film of PcCu (approximately 15 – 30 nm), a thicker film (approximately 100 – 150 nm) of the emitter and finally the air-stable aluminium cathode was evaporated in high vacuum (1×10^{-5} mbar). For a screening-test of the electroluminescent properties, the glass-ITO substrates contained 25 segments (0.4 cm × 0.8 cm). Each segment was driven separately. For EL measurements, a HP6030A voltage source was used together with a Keithley 171 DMM. EL spectra were taken with a waveguide/diode array set-up. The emitted light was harvested for 30 s at voltages between 14 and 20 V, dependent on the thickness of the device segment and the strength of the emitter. All UV/Vis, PL and EL data were measured in air at room temperature.

Synthesis of monoaldehydes 11 and 13:[13] $TiCl_4$ (1 mL, 9 mmol) was added to a solution of the aromatic dihexyloxy compound (5 mmol) in dichloromethane (100 mL) at 0 °C with a syringe, followed by addition of dichloromethyl methyl ether (1 mL, 11 mmol). After 15 min at room temperature the reaction was carefully hydrolyzed with water (40 mL). The organic phase was washed again with water (30 mL), saturated $NaHCO_3$ (40 mL) and brine (50 mL), and dried over magnesium sulfate. After evaporation of the solvent, the crude product was purified by column chromatography (silica gel, hexane/dichloromethane).

General procedure for the Knoevenagel reaction:[4a] As an example, dialdehyde **7** (0.3 mmol) and cyanomethylene compound **12** (0.6 mmol) were dissolved in a mixture of THF (1 mL) and *t*BuOH (2 mL) under an argon atmosphere. A drop of tetra-*n*-butyl ammonium hydroxide and anhydrous potassium *tert*-butoxide (0.05 mmol) were added, and the mixture was stirred vigorously while warmed to 40 °C. After 20 min the mixture was poured into methanol (50 mL, acidified with a drop of acetic acid) to precipitate the compound. The product was redissolved in dichloromethane, precipitated with methanol and the solid recrystallized from a methanol/dichloromethane mixture.

***E*-1,4-Bis(*β*-cyano-2′,5′-di-*n*-hexyloxystyryl)-2,5-di-*n*-hexyloxybenzene (21)**: Yield: 44 %; ^{1}H NMR: $\delta = 7.92$ (s, 2H), 7.74 (d, $J = 2.7$ Hz, 2H), 6.98 (s, 2H), 6.88 (dd, $J = 9.1$, 2.7 Hz, 2H), 6.78 (d, $J = 9.1$ Hz, 2H), 3.97 (t, $J = 6.4$ Hz, 4H), 3.93 (t, $J = 6.4$ Hz, 4H), 3.89 (t, $J = 6.4$ Hz, 4H), 1.85 – 1.60 (m, 12H), 1.50 – 1.10 (m, 36H), 0.83 (t, $J = 7.0$ Hz, 6H), 0.79 (t, $J = 6.7$ Hz, 6H), 0.78 (t, $J = 6.7$ Hz, 6H); ^{13}C NMR: $\delta = 152.9$, 151.8, 150.6, 141.8, 126.1, 123.7, 119.2, 118.3, 114.6, 113.3, 113.2, 107.8, 69.8, 69.3, 68.8, 31.7, 31.6, 29.7, 29.3, 29.2, 25.8, 22.6, 14.1, 14.0; IR (KBr): $\tilde{\nu} = 2932$, 2210, 1506, 1474, 1260, 1215, 1026, 800 cm^{-1}; m.p. 139.8 – 141.5 °C; UV/Vis (CH_2Cl_2): $\lambda = 261$, 282, 302, 384 nm; PL (solid state): 485 nm.

***E*-1,4-Bis(*α*-cyano-2′,5′-di-*n*-hexyloxystyryl)-2,5-di-*n*-hexyloxybenzene (22)**: Yield: 46 %; ^{1}H NMR: $\delta = 7.88$ (s, 2H), 7.82 (s, 2H), 6.94 (t, $J = 1.5$ Hz, 2H), 6.81 (d, $J = 1.5$ Hz, 4H), 4.02 (t, $J = 6.4$ Hz, 4H), 3.94 (t, $J = 6.7$ Hz, 4H), 3.87 (t, $J = 6.5$ Hz, 4H), 1.73 (t, $J = 7.0$ Hz, 12H), 1.47 – 1.15 (m, 36H), 0.84 (t, $J = 7.0$ Hz, 6H), 0.79 (t, $J = 7.0$ Hz, 12H); ^{13}C NMR: $\delta = 153.2$, 151.3, 150.8, 140.3, 125.9, 125.7, 118.5, 116.1, 116.0, 114.0, 111.4, 109.0, 69.7, 69.3, 68.8, 31.6, 31.5, 29.3, 29.2, 25.8, 25.7, 22.6, 22.5, 14.0, 13.95, 13.90; IR (KBr): $\tilde{\nu} = 2943$, 2870, 2208, 1504, 1470, 1230, 1060, 802 cm^{-1}; m.p. 85.5 – 86.8 °C; UV/Vis (CH_2Cl_2): $\lambda = 328$, 418 nm; PL (solid state): 512 nm.

***E*-1,4-Bis(*β*-cyano-*α*-1′,4′-di-*n*-hexyloxynaphth-2-ylvinyl)-2,5-di-*n*-hexyloxybenzene (23)**: Yield: 72 %; ^{1}H NMR: $\delta = 8.25 – 8.18$ (m, 2H), 8.08 (s, 2H), 8.04 – 8.00 (m, 2H), 7.70 (s, 2H), 7.50 (t, $J = 3.3$ Hz, 2H), 7.46 (t, $J = 3.3$ Hz, 2H), 7.06 (s, 2H), 4.19 (t, $J = 6.2$ Hz, 4H), 4.03 (t, $J = 6.6$ Hz, 4H), 3.89 (t, $J = 6.6$ Hz, 4H), 1.94 – 1.70 (m, 12H), 1.60 – 1.12 (m, 36H), 0.85 (t, $J = 6.8$ Hz, 6H), 0.79 (t, $J = 7.0$ Hz, 6H), 0.75 (t, $J = 6.9$ Hz, 6H); ^{13}C NMR: $\delta = 151.2$, 150.7, 149.8, 141.9, 128.6, 128.3, 126.9, 126.3, 122.9, 122.7, 118.5, 114.5, 107.7, 101.9, 76.5, 69.9, 68.5, 31.7, 31.65, 31.6, 30.4, 29.3, 29.2, 26.0, 25.9, 25.8, 22.6, 22.5, 14.1, 14.05, 14.0; IR (KBr): $\tilde{\nu} = 2950$, 2212, 1597, 1504, 1391, 1236, 1094, 770 cm^{-1}; m.p. 128.4 – 130.2 °C; UV/Vis (CH_2Cl_2): $\lambda = 291$, 397 nm; PL (solid state): 510 nm.

***E*-1,4-Bis(*α*-cyano-*α*-1′,4′-di-*n*-hexyloxynaphth-2-ylvinyl)-2,5-di-*n*-hexyloxybenzene (24)**: Yield: 53 %; ^{1}H NMR: $\delta = 8.21$ (dm, $J = 7.3$ Hz, 2H), 8.10 (s, 2H), 8.07 (dm, $J = 7.3$ Hz, 2H), 7.93 (s, 2H), 7.48 (dq, $J = 7.0$ Hz, 1.5 Hz, 4H), 6.76 (s, 2H), 4.09 (t, $J = 6.1$ Hz, 4H), 4.07 (t, $J = 6.1$ Hz, 4H), 3.89 (t, $J = 6.7$ Hz, 4H), 1.94 – 1.69 (m, 12H), 1.60 – 1.15 (m, 36H), 0.86 (t, $J = 6.7$ Hz, 6H), 0.79 (t, $J = 7.0$ Hz, 6H), 0.78 (t, $J = 6.7$ Hz, 6H); ^{13}C NMR: $\delta = 151.5$ (2 signals), 146.9, 140.9, 129.2, 127.05, 127.0, 126.3, 126.0, 123.7, 122.6, 122.4, 118.7, 111.3, 108.8, 104.4, 75.1, 69.4, 68.5, 31.7, 31.6, 31.5, 30.3, 29.3, 29.2, 25.9, 25.85, 25.8, 22.6, 22.5, 14.0, 13.9; IR (KBr): $\tilde{\nu} = 2953$, 2214, 1472, 1425, 1369, 1211, 1099, 766 cm^{-1}; m.p. 105.8 – 106.3 °C; UV/Vis (CH_2Cl_2): $\lambda = 313$, 438 nm; PL (solid state): 560 nm.

***E*-2,6-Bis(*β*-cyano-2′,5′-di-*n*-hexyloxystyryl)-1,5-di-*n*-hexyloxynaphthalene (25)**: Yield: 82 %; ^{1}H NMR: $\delta = 8.03$ (s, 2H), 7.93 (d, $J = 8.5$ Hz, 2H), 7.82 (d, $J = 3.0$ Hz, 2H), 7.54 (d, $J = 8.5$ Hz, 2H), 6.91 (dd, $J = 9.1$ Hz, 3.0 Hz, 2H), 6.80 (d, $J = 9.1$ Hz, 2H), 3.95 (t, $J = 6.4$ Hz, 8H), 3.91 (t, $J = 6.4$ Hz, 4H), 1.89 – 1.65 (m, 12H), 1.58 – 1.15 (m, 36H), 0.84 (t, $J = 6.7$ Hz, 6H), 0.79 (t, $J = 6.7$ Hz, 6H), 0.78 (t, $J = 6.7$ Hz, 6H); ^{13}C NMR: $\delta = 153.5$, 152.9, 151.9, 142.4, 130.2, 127.1, 125.5, 123.5, 119.3, 119.1, 118.4, 113.3, 112.9, 107.4, 75.2, 69.3, 68.8, 31.7, 31.6, 31.5, 30.2, 29.3, 29.2, 25.7, 22.6, 22.5, 14.0, 13.95, 13.9; IR (KBr): $\tilde{\nu} = 2930$, 2210, 1497, 1470, 1223, 1015 cm^{-1}; m.p. 71.5 – 72.1 °C; UV/Vis (CH_2Cl_2): $\lambda = 294$, 379 nm; PL (solid state): 477 nm.

***E*-2,6-Bis(*α*-cyano-2′,5′-di-*n*-hexyloxystyryl)-1,5-di-*n*-hexyloxynaphthalene (26)**: Yield: 59 %; ^{1}H NMR: $\delta = 8.31$ (d, $J = 9.1$ Hz, 2H), 7.98 (s, 2H), 7.90 (d, $J = 9.1$ Hz, 2H), 6.99 (t, $J = 1.5$ Hz, 2H), 6.83 (d, $J = 1.5$ Hz, 4H), 3.96 (t, $J = 6.7$ Hz, 4H), 3.95 (t, $J = 6.7$ Hz, 4H), 3.88 (t, $J = 6.7$ Hz, 4H), 1.89 – 1.65 (m, 12H), 1.53 – 1.17 (m, 36H), 0.84 (t, $J = 7.0$ Hz, 6H), 0.80 (t, $J = 7.0$, 6H), 0.76 (t, $J = 7.0$ Hz, 6H); ^{13}C NMR: $\delta = 155.9$, 153.3, 150.8, 140.9, 130.4, 125.4, 125.2, 119.1, 118.3, 116.3, 116.0, 114.0, 110.2, 77.0, 69.7, 68.8, 31.7, 31.65, 31.60, 30.4, 29.3, 29.2, 25.8, 25.7, 22.6, 14.1, 14.0; IR (KBr): $\tilde{\nu} = 2932$, 2214, 1499, 1468, 1229, 1036, 806 cm^{-1}; m.p. 74.6 – 77.2 °C; UV/Vis (CH_2Cl_2): $\lambda = 291$, 342, 399 nm; PL (solid state): 510 nm.

***E*-2,6-Bis(*β*-cyano-*α*-1′,4′-di-*n*-hexyloxynaphth-2-ylvinyl)-1,5-di-*n*-hexyloxynaphthalene (27)**: Yield: 76 %; ^{1}H NMR: $\delta = 8.28 – 8.21$ (m, 2H), 8.17 (s, 2H), 8.07 – 8.00 (m, 2H), 7.99 (d, $J = 8.8$ Hz, 2H), 7.81 (s, 2H), 7.60 (d, $J = 8.5$ Hz, 2H), 7.54 – 7.46 (m, 4H), 4.22 (t, $J = 6.2$ Hz, 4H), 3.99 (t, $J = 6.7$ Hz, 4H), 3.91 (t, $J = 6.5$ Hz, 4H), 1.97 – 1.74 (m, 12H), 1.62 – 1.15 (m, 36H), 0.86 (t, $J = 7.0$ Hz, 6H), 0.74 (t, $J = 7.0$ Hz, 12H); ^{13}C-NMR: $\delta = 153.6$, 151.3, 150.1, 142.5, 130.4, 128.6, 128.4, 127.2, 127.1, 127.0, 125.9, 122.9, 122.7, 119.3, 118.6, 107.2, 101.5, 77.2, 75.3, 68.6, 31.6, 30.3, 30.2, 29.3, 26.0, 25.9, 25.8, 22.6, 22.55, 22.50, 14.0, 13.9; IR (KBr): $\tilde{\nu} = 2934$, 2210, 1468, 1380, 1252, 1092, 762 cm^{-1}; m.p. 118.4 – 120.2 °C; UV/Vis (CH_2Cl_2): $\lambda = 295$, 398 nm; PL (solid state): 482 nm.

***E*-2,6-Bis(*α*-cyano-*α*-1′,4′-di-*n*-hexyloxynaphth-2-ylvinyl)-1,5-di-*n*-hexyloxynaphthalene (28)**: Yield: 93 %; ^{1}H NMR: $\delta = 8.44$ (d, $J = 8.8$ Hz, 2H), 8.23 (dm, $J = 6.7$ Hz, 2H), 8.16 (s, 2H), 8.08 (dm, $J = 6.7$ Hz, 2H), 7.97 (d, $J = 8.8$ Hz, 2H), 7.56 – 7.44 (m, 4H), 6.80 (s, 2H), 4.11 (t, $J = 6.4$ Hz, 4H), 3.98 (t, $J = 6.4$ Hz, 4H), 3.91 (t, $J = 6.4$ Hz, 4H), 1.95 – 1.73 (m, 12H), 1.60 – 1.10 (m, 36H), 0.86 (t, $J = 7.0$ Hz, 6H), 0.74 (t, $J = 7.0$ Hz, 6H), 0.73 (t, $J = 7.0$ Hz, 6H); ^{13}C NMR: $\delta = 156.1$, 151.6, 147.0, 141.5, 130.5, 129.2, 127.1, 126.4, 125.1, 124.9, 123.7, 122.7, 122.5, 119.3, 118.5, 109.7, 104.2, 77.3, 75.2, 68.5, 31.7, 31.6, 30.4, 30.3, 29.3, 26.0, 25.9, 25.8, 22.6, 22.5, 14.0, 13.95,13.90; IR (KBr): $\tilde{\nu} = 2930$, 2216, 1506, 1404, 1227, 1101, 771 cm^{-1}; m.p. 163.0 – 164.8 °C; UV/Vis (CH_2Cl_2): $\lambda = 297$, 349, 411 nm; PL (solid state): 506 nm.

0947-6539/00/0608-1300 $ 17.50+.50/0 *Chem. Eur. J.* **2000**, *6*, No. 8

Acknowledgement

We thank the Fonds der Chemischen Industrie for the financial support of this work.

[1] a) A. Kraft, A. C. Grimsdale, A. B. Holmes, *Angew. Chem*. **1998**, *110*, 416; *Angew. Chem. Int. Ed. Engl.* **1998**, *37*, 402; b) J. Salbeck, *Ber. Bunsenges. Phys. Chem*. **1996**, *100*, 1667; c) J. L. Segura, *Acta Polym.* **1998**, *49*, 319.

[2] G. Gustafsson, Y. Cao, G. M. Treacy, F. Klavetter, N. Colaneri, A. J. Heeger, *Nature* **1992**, *357*, 477.

[3] N. C. Greenham, S. C. Moratti, D. D. C. Bradley, R. H. Friend, A. B. Holmes, *Nature* **1993**, *365*, 628.

[4] a) S. C. Moratti, R. Cervini, A. B. Holmes, D. R. Baigent, R. H. Friend, N. C. Greenham, J. Grüner, P. J. Hamer, *Synth. Met*. **1995**, *71*, 2117; b) H. Hong, D. Davidov, Y. Avny, H. Chayet, E. Z. Faraggi, R. Neumann, *Adv. Mater*. **1995**, *7*, 846.

[5] M. Hanack, J. L. Segura, H. Spreitzer, *Adv. Mater*. **1996**, *8*, 663.

[6] M. Hohloch, J. L. Segura, S. E. Döttinger, D. Hohnholz, E. Steinhuber, H. Spreitzer, M. Hanack, *Synth. Met*. **1997**, *84*, 319.

[7] S. C. Moratti, R. Cervini, A. B. Holmes, D. R. Baigent, R. H. Friend, *Synth. Met*. **1995**, *71*, 2117.

[8] E. Z. Faraggi, H. Chayet, G. Cohen, R. Neumann, Y. Avny, D. Davidov, *Adv. Mater*. **1995**, *7*, 742.

[9] S. Tasch, W. Graupner, G. Leising, Lin Pu, M. W. Wagner, R. H. Grubbs, *Adv. Mater.* **1995**, *7*, 903.

[10] a) S. E. Döttinger, M. Hohloch, J. L. Segura, E. Steinhuber, M. Hanack, A. Tompert, D. Oelkrug, *Adv. Mater*. **1997**, *9*, 233; b) S. E. Döttinger, M. Hohloch, D. Hohnholz, J. L Segura, E. Steinhuber, M. Hanack, *Synth. Met.* **1997**, *84*, 267; c) J. L. Segura, N. Martin, M. Hanack, *Eur. J. Org. Chem.* **1999**, 643.

[11] M. Hohloch, C. Maichle-Mössmer, M. Hanack, *Chem. Mater*. **1998**, *10*, 1327.

[12] a) S. A. Van Slyke, C. H. Chen, C. W. Tang, *Appl. Phys. Lett.* **1996**, *69*, 216; b) D. Hohnholz, S. Steinbrecher, M. Hanack, *J. Mol. Struct.*, in press.

[13] a) L. N. Ferguson, *Chem. Rev.* **1946**, *38*, 231; b) A. Rieche, H. Gross, E. Höft, *Org. Synth.* **1967**, *5*, 49.

[14] M. Gates, *J. Org. Chem*. **1982**, *47*, 579.

[15] a) J. Cornil, D. A. dos Santos, D. Beljonne, J. L. Brédas, *J. Phys. Chem.* **1995**, *99*, 5604; b) J. L. Brédas, *Adv. Mater.* **1995**, *7*, 263; c) J. L. Brédas, A. J. Heeger, *Chem. Phys. Lett.* **1994**, *217*, 507.

[16] a) D. Oelkrug, A. Tompert, H.-J. Egelhaaf, M. Hanack, E. Steinhuber, M. Hohloch, H. Meier, U. Stalmach, *Synth. Met.* **1996**, *83*, 231; b) D. Oelkrug, A. Tompert, J. Gierschner, H.-J. Egelhaaf, M. Hanack, M. Hohloch, E. Steinhuber, *J. Phys. Chem. B* **1998**, *102*, 1902.

[17] I. D. W. Samuel, G. Rumbles, C. J. Collison, *Phys. Rev. B* **1995**, *52*, R11573.

[18] D. Hohnholz, K.-H. Schweikart, M. Hanack, *Adv. Mater.* **1999**, *8*, 646.

Received: August 5, 1999 [F1961]